

# Comparison of detrending methods for fluctuation analysis

Amir Bashan<sup>a</sup>, Ronny Bartsch<sup>a,\*</sup>, Jan W. Kantelhardt<sup>b</sup>, and Shlomo Havlin<sup>a</sup>

<sup>a</sup>*Minerva Center, Dept. of Physics, Bar-Ilan University, Ramat-Gan 52900, Israel*

<sup>b</sup>*Institute of Physics, Martin-Luther-Universität Halle-Wittenberg, 06099 Halle, Germany*

submitted: 22 August 2007; accepted: 31 March 2007

---

## Abstract

We examine several recently suggested methods for the detection of long-range correlations in data series based on similar ideas as the well-established Detrended Fluctuation Analysis (DFA). In particular, we present a detailed comparison between the regular DFA and two recently suggested methods: the Centered Moving Average (CMA) Method and a Modified Detrended Fluctuation Analysis (MDFA). We find that CMA is performing equivalently as DFA in long data with weak trends and slightly superior to DFA in short data with weak trends. When comparing standard DFA to MDFA we observe that DFA performs slightly better in almost all examples we studied. We also discuss how several types of trends affect the different types of DFA. For weak trends in the data, the new methods are comparable with DFA in these respects. However, if the functional form of the trend in data is not a-priori known, DFA remains the method of choice. Only a comparison of DFA results, using different detrending polynomials, yields full recognition of the trends. A comparison with independent methods is recommended for proving long-range correlations.

*Key words:* time series analysis, long-range correlations, detrended fluctuation analysis, crossovers, non-stationarities

*PACS:* 05.40.-a, 05.45.Tp

---

\* Corresponding author. Tel.: + 972 3 5317885; fax: + 972 3 5317884.  
*Email address:* bartsch.ronny@gmail.com (Ronny Bartsch).

## 1 Introduction

Experimental data are often affected by non-stationarities, i.e. varying mean and standard deviation. These effects have to be well distinguished from the intrinsic fluctuations and correlations of the system in order to find the correct scaling behaviour. Sometimes we do not know the reasons for underlying non-stationarities in collected data and – even worse – we do not know the type of the underlying non-stationarities.

In the last decade *Detrended Fluctuation Analysis* (DFA), originally introduced by Peng et al. [1], has been established as an important method to reliably detect long-range (auto-) correlations<sup>1</sup> in data effected by trends. The method is based on random walk theory. Its non-detrending predecessors are Hurst’s rescaled range analysis [2] and fluctuation analysis (FA) [3]. DFA was later generalized for higher order detrending [4], multifractal analysis [5], separate analysis of sign and magnitude series [6], and data with more than one dimension [7]. Its features have been studied in many articles [8,9,10,11,12,13]. In addition, several comparisons of DFA with other methods for stationary and non-stationary time-series analysis have been published, see, e.g., [14,15,16,17] and in particular [18], where DFA is compared with many other established methods for short data sets.

The convenience of DFA has led to a broad range of application in very diverse fields where long-range correlations are of interest:

- DNA sequences,
- medical and physiological time series (recordings of heartbeat, breathing, blood pressure, blood flow, nerve spike intervals, human gait, glucose levels, gene expression data),
- geophysics time series (recordings of temperature, precipitation, water runoff, ozone levels, wind speed, seismic events, vegetational patterns, and climate dynamics),
- astrophysical time series (X-ray light sources and sunspot numbers),
- technical time series (internet traffic, highway traffic, and neutronic power from a reactor),
- social time series (finance and economy, language characteristics, fatalities in the Iraq conflict), as well as
- physics data, e.g., surface roughness, chaotic spectra of atoms, and photon correlation spectroscopy recordings.

Altogether, there are about 450 papers applying DFA. In most cases positive auto-correlations were reported leaving only a few exceptions with anti-

---

<sup>1</sup> In the following we will label long-range as long-term when speaking, more specifically, about time series.

correlations, see, e.g., [19,20,21].

In the DFA technique – as in all techniques based on random walk theory – time series are integrated by partial summation which enables also the analysis of data with weak correlations. In addition the integration reduces the noise level caused by imperfect measurements and noise, an advantage that applies also to other related non-detrending methods [2,3]. However, for the reliable characterization of time series, it is also essential to distinguish trends from intrinsic fluctuations, that might be long-term correlated. Monotonous, periodic or step-like trends are caused by external effects, e. g., by the greenhouse warming [22], seasonal variations for temperature records [23] and river runoffs [2,24,25,26], different levels of daily activity in long-term physiological data [27], or unstable light sources in photon correlation spectroscopy [28]. To characterize a complex system based on time series, trends and fluctuations are usually studied separately (see, e.g., [29] for a recent discussion). Strong trends in data can lead to a false detection of long-term correlations if only one (non-detrending) method is used or if the results are not carefully interpreted. A major advantage of the DFA technique is the systematic elimination of polynomial trends of different order [4,8,9]. Note however that an additive composition of fluctuations and trends is assumed. The technique can thus assist in gaining insight into the scaling behaviour of the natural variability as well as into the kind of trends of the considered time series [30].

Still, we would like to note that conclusions should not be based on DFA or variants of this method alone in most applications. In particular, if it is not clear whether a given time series is indeed long-term correlated or just short-term correlated with a fairly large correlation time scale, results of DFA should be compared with other methods. For example, one can employ wavelet methods (see, e.g., [23,25,31,32,33]). Another option is to remove short-term correlations by considering averaged series for comparison. For a time series with daily observations and possible short-term correlations up to two years, for example, one might consider the series of two-year averages and apply DFA as well as FA, Hurst's Analysis, binned power spectra analysis, and/or wavelet analysis. Only if at least two independent methods consistently indicate long-term correlations, one can be sure that the data are indeed long-term correlated.

Lately, several modifications of the DFA method have been suggested with many different techniques for the elimination of monotonous and periodic trends. These methods include

- the Detrended Moving Average technique [34,35,36], which we denote by Backward Moving Average (BMA) technique (following [37]),
- the Centered Moving Average (CMA) method [37], an essentially improved version of BMA,

- the Modified Detrended Fluctuation Analysis (MDFA) [38], which is essentially a mixture of old FA and DFA,
- the continuous DFA (CDFA) technique [39,40], which is particularly intended for the detection of transitions,
- the Fourier DFA [41],
- a variant of DFA based on empirical mode decomposition (EMD) [42],
- a variant of DFA based on singular value decomposition (SVD) [43,44], and
- a variant of DFA based on high-pass filtering [45].

Although several of the original publications compare their new suggested method with the DFA, there is no inter-comparison between these new methods. Hence, it is not clear which methods might be most suitable for which application. In this work we comment on all recently suggested detrending random walk based methods we are aware of. Moreover, we study and compare in detail two of the most prominent and – according to our studies – most suitable new methods with standard DFA, presenting their advantages and disadvantages. For recent comparative studies not focused on detrending methods, see [14,17,18]. For studies comparing DFA and BMA, see [46,47]; note that [47] also discusses CMA. For studies comparing methods for detrending multifractal analysis (multifractal DFA (MF-DFA) and wavelet transform modulus maxima (WTMM) method), see [5,24,48].

The paper is organized as follows: In Section 2 we thoroughly explain the standard DFA as well as the Centered Moving Average (CMA) method, and a Modified Detrended Fluctuation Analysis (MDFA). We further introduce several other (more complicated) detrending methods and remark on their utility. Section 3 reports and discusses our results for DFA, CMA and MDFA, obtained from monofractal artificial time series with different lengths, crossovers and monotonous trends. We conclude in Section 4.

## 2 Methods

### 2.1 Long-Range Correlations

We consider a record  $(x_i)$  of  $i = 1, \dots, N$  equidistant measurements. In most applications, the index  $i$  will correspond to the time of the measurements. We are interested in the correlation of the values  $x_i$  and  $x_{i+s}$  for different time lags, i. e. correlations over different time scales  $s$ . In order to remove a constant offset in the data, the mean  $\langle x \rangle = \frac{1}{N} \sum_{i=1}^N x_i$  is usually subtracted,  $\tilde{x}_i \equiv x_i - \langle x \rangle$ . Quantitatively, correlations between  $x$ -values separated by  $s$

steps are defined by the (auto-) correlation function

$$C(s) = \frac{\langle \tilde{x}_i \tilde{x}_{i+s} \rangle}{\langle \tilde{x}_i^2 \rangle} = \frac{1}{(N-s)\langle \tilde{x}_i^2 \rangle} \sum_{i=1}^{N-s} \tilde{x}_i \tilde{x}_{i+s}. \quad (1)$$

If the  $x_i$  are uncorrelated,  $C(s)$  is zero for  $s > 0$ . Short-range correlations of the  $x_i$  are described by  $C(s)$  declining exponentially,  $C(s) \sim \exp(-s/t_\times)$  with a decay time  $t_\times$ . For so-called *long-range correlations*,  $t_\times = \int_0^\infty C(s) ds$  diverges and the decay time  $t_\times$  cannot be defined. For example,  $C(s)$  declines as a power-law

$$C(s) \sim s^{-\gamma} \quad (2)$$

with an exponent  $0 < \gamma < 1$ . A direct calculation of  $C(s)$  is usually not appropriate due to underlying non-stationarities and trends of unknown origin. Furthermore,  $C(s)$  strongly fluctuates around zero on large scales  $s$ , making it impossible to find the potential scaling behaviour (2). Thus, one has to determine the correlation exponent  $\gamma$  indirectly.

Note that in some applications a separate inspection of short-term and long-term correlations is desirable. A convenient way to exclude short-term correlations up to a scale  $s_l$  is downsampling the original data by the same factor  $s_l$ . Contrariwise, the segmentation of the data into boxes of length  $s_u$  and a subsequent shuffling of the boxes destroys long-term correlations on scales above  $s_u$ .

## 2.2 Detrended Fluctuation Analysis (DFA)

The method of *Detrended Fluctuation Analysis* (DFA) [1] is an improvement of classical fluctuation analysis (FA) [3], which is similar to Hurst's rescaled range ( $R/S$ -) analysis [2]. They allow determining the correlation properties on large time scales. All three methods are based on random walk theory. One first calculates the 'profile'

$$X(n) = \sum_{i=1}^n (x_i - \langle x \rangle) \quad (3)$$

of a time series  $(x_i)$ ,  $i = 1, \dots, N$  (with mean  $\langle x \rangle$ ), which can be considered as the position of a random walker on a linear chain after  $n$  steps.

Then the profile is divided into  $N_s \equiv [N/s]$  non-overlapping segments of equal length ('scale')  $s$ . The mean-squared fluctuation function of the FA method is

given by

$$F^2(s) = \frac{1}{N_s} \sum_{\nu=1}^{N_s} [X((\nu-1)s) - X(\nu s)]^2. \quad (4)$$

In Hurst's  $R/S$  analysis (see [17] and references therein for a recently suggested improved version and tests), one calculates in each segment  $\nu$  the range  $R$  of  $X(n)$  given by the difference between maximal and minimal value,  $R(s) = X_{\max} - X_{\min}$ . The "rescaling of range" is done by dividing  $R(s)$  by the corresponding standard deviation  $S(s) = \sigma(X(n))$  of the same segment  $\nu$ . The mean of all quotients at a particular scale  $s$  is equivalent to  $F(s)$  (except for multi-fractal data) and usually shows a power-law scaling relationship with  $s$ .

While both, FA and Hurst's method fail to determine correlation properties if linear or higher order trends are present in the data, DFA explicitly deals with monotonous trends in a detrending procedure. This is done by estimating a piecewise polynomial trend  $y_s^{(p)}(n)$  within each segment  $\nu$  by least-square fitting. I.e.,  $y_s^{(p)}(n)$  consists of concatenated polynomials of order  $p$  which are calculated separately for each of the segments. The detrended profile function  $\tilde{X}_s(n)$  on scale  $s$  is determined by ('detrending'):

$$\tilde{X}_s(n) = X(n) - y_s^{(p)}(n). \quad (5)$$

The degree of the polynomial can be varied in order to eliminate linear ( $p = 1$ ), quadratic ( $p = 2$ ) or higher order trends of the profile function [4]. Conventionally the DFA is named after the order of the fitting polynomial (DFA1, DFA2, ...). Note that DFA1 is equivalent to Hurst's analysis in terms of detrending.

The variance of  $\tilde{X}_s(n)$  yields the fluctuation function on scale  $s$

$$F(s) = \left\{ \frac{1}{N} \sum_{n=1}^N \tilde{X}_s^2(n) \right\}^{1/2}. \quad (6)$$

This function, which has to be calculated for different scales  $s$ , corresponds to the trend-eliminated root mean square displacement of the random walker mentioned above and is related to the auto-correlation function by an integral expression [1]; see the appendix of [14] for a derivation for DFA1. For an equivalent, but more common description of DFA, see, e.g., [8]. We note that in studies that include averaging over many records (or one record cut into many separate pieces by the elimination of some unreliable intermediate data points) the averaging procedure (6) must be performed for all data. Taking the square root should usually be the final step after all averaging is finished; however note [16,17], where this order is reversed. It is usually not appropriate

to calculate  $F(s)$  for parts of the data and then average the  $F(s)$  values, since such a procedure will bias the results towards smaller scaling exponents on large time scales close to the maximum scale  $s_{\max} \approx N/4$  where statistically reliable results can be obtained [8].

If  $F(s)$  increases for increasing  $s$  asymptotically as

$$F(s) \sim s^\alpha \tag{7}$$

with  $0.5 < \alpha < 1$ , one finds that the scaling (or 'Hurst') exponent  $\alpha$  is related to the correlation exponent  $\gamma$  by  $\alpha = 1 - \gamma/2$  [14]. A value of  $\alpha = 0.5$  thus indicates that there are no (or only short-term) correlations. If  $\alpha > 0.5$ , the data are long-term correlated. The higher  $\alpha$ , the stronger are the correlations in the signal. Note that  $\alpha > 1$  indicates a non-stationary local average of the data; in this case both, FA and Hurst analysis fail and yield only  $\alpha = 1$ . The case  $\alpha < 0.5$  corresponds to long-term anticorrelations, meaning that large values are most likely to be followed by small values and vice versa [19,20,21].

If the type of trends in given data is not known beforehand, the fluctuation function  $F(s)$  should be calculated for several orders  $p$  of the fitting polynomial. If  $p$  is too low,  $F(s)$  will show a pronounced crossover to a regime with larger slope for large scales  $s$  [8,9]. The maximum slope of  $\log F(s)$  versus  $\log s$  is  $p + 1$ . The crossover will move to larger scales  $s$  or disappear when  $p$  is increased, unless it is a real crossover in the intrinsic fluctuations and not due to trends [8]. Hence, one can find  $p$  such that detrending is sufficient. However,  $p$  should not be larger than necessary, because deviations on short scales  $s$  increase with increasing  $p$ .

### 2.3 Centered Moving Average (CMA) Analysis

A possible drawback of the DFA method is the occurrence of abrupt jumps in the detrended profile  $\tilde{X}_s(n)$  (Eq. (5)) at the boundaries between the segments, since the fitting polynomials in neighbouring segments are not related. A simple way to avoid these jumps would be the calculation of  $F(s)$  based on polynomial fits in overlapping windows. However, this is rather time consuming due to the polynomial fit in each segment and is consequently not done in most applications. To overcome the problem of artificial jumps and to reliably determine the scaling exponent  $\alpha$  in non-stationary time series, several modifications of the FA and DFA methods were suggested in the last years.

A particular attractive modification leads to the methods of *Detrended Moving Average* (DMA), where running averages replace the polynomial fits. Its first suggested version, the *Backward Moving Average* (BMA) method [34,35,36],

however, slightly underestimates the scaling exponent by about 0.05, because an artificial time shift of  $s$  between the original signal and the moving average is introduced. This time shift leads to an additional contribution to  $\tilde{X}_s(n)$ , which causes a larger fluctuation function  $F(s)$  in particular for small scales in the case of long-term correlated data [46]. In addition, the BMA method is effectively not detrending [47]. Its slope  $\alpha$  is limited by 1 just as for the earlier non-detrending methods FA and  $R/S$ .

It was soon recognized that the artificial time shift of the BMA method can easily be eliminated. This leads to the *Centered Moving Average* (CMA) method [37], where  $\tilde{X}_s(n)$  is calculated as

$$\tilde{X}_s(n) = X(n) - \frac{1}{s} \sum_{j=-(s-1)/2}^{(s-1)/2} X(n+j), \quad (8)$$

while Eq. (6) stays the same. Unlike DFA, the CMA method cannot easily be generalized to remove linear and higher order trends in the data. However, CMA is somehow similar to DFA1 with overlapping windows.

#### 2.4 Modified Detrended Fluctuation Analysis (MDFA)

Another type of detrended fluctuation analysis, which we will denote as *Modified Detrended Fluctuation Analysis* (MDFA) [38], eliminates trends similar to the DFA method. A polynomial is fitted to the profile function  $X(n)$  in each segment  $\nu$  and the deviation between the profile function and the polynomial fit is calculated,  $\tilde{X}_s(n) = X(n) - y_s^{(p)}(n)$ . To estimate correlations in the data, this method uses a derivative of  $\tilde{X}_s(n)$ , obtained for each segment  $\nu$ , by  $\Delta\tilde{X}_s(n) = \tilde{X}_s(n+s/2) - \tilde{X}_s(n)$ . Hence, Eq. (6) becomes

$$F(s) = \left\{ \frac{1}{N} \sum_{n=1}^N [\Delta\tilde{X}_s(n)]^2 \right\}^{1/2}. \quad (9)$$

As in case of DFA, MDFA can easily be generalized to remove higher order trends in the data. Since the fitting polynomials in adjacent segments are not related,  $\Delta\tilde{X}_s(n)$  shows abrupt jumps on their boundaries as well. This leads to fluctuations of  $F(s)$  for large segment sizes  $s$  as we will show below.



## 2.5 Further Modifications and Extensions of DFA

Several modifications and extensions of DFA have been proposed. Most of them are, however, rather complicated in implementation. While they might be very useful in particular applications, we believe the implications of the complicated detrending and decomposition techniques are not sufficiently understood and their programming effort is too large for a wide usage.

The *Fourier-detrended fluctuation analysis* [41] aims to eliminate slow oscillatory trends which are found especially in weather and climate series due to seasonal influences. The character of these trends can be rather periodic and regular or irregular, and their influence on the detection of long-range correlations by means of DFA was systematically studied previously [8]. Among other things it has been shown that low-frequency periodic trends disturb the scaling behaviour of the results much stronger than high-frequency trends and thus have to be removed prior to the analysis. In case of periodic and regular oscillations, e.g., in temperature fluctuations one simply removes the low frequency seasonal trend by subtracting the daily mean temperatures from the data. Another way, which the Fourier-detrended fluctuation analysis suggests, is to filter out the relevant frequencies in the signals' Fourier spectrum before applying DFA to the filtered signal. Nevertheless, this method which is only an extension of DFA faces several difficulties especially its limitation to periodic and regular trends. Furthermore one needs to know the interfering frequency band beforehand.

To study correlations in data with quasi-periodic or irregular oscillating trends, *empirical mode decomposition* (EMD) was suggested [42]. The EMD algorithm breaks down the signal into its intrinsic mode functions (IMFs) which can be used to distinguish between fluctuations and trends. The trends, estimated by a quasi-periodic fit containing the dominating frequencies of a sufficiently large number of IMFs, is subtracted from the data, yielding a slightly better scaling behaviour in the DFA curves. However, we believe, that this extension of DFA is too complicated for wide-spread applications.

Another extension of DFA which was shown to minimize the effect of periodic and quasi-periodic trends is based on *singular value decomposition* (SVD) [43,44]. In this approach, one first embeds the original signal in a matrix whose dimension has to be much larger than the number of frequency components of the periodic or quasi-periodic trends obtained in the power spectrum. Applying SVD yields a diagonal matrix which can be manipulated by setting the dominant eigen-values (associated with the trends) to zero. The filtered matrix finally leads to the filtered data, and it has been shown that subsequent application of DFA determines the expected scaling behaviour if the embedding dimension is sufficiently large. None the less, the performance of

this rather complex method seems to decrease for larger values of the scaling exponent. Furthermore SVD-DFA assumes that trends are deterministic and narrow banded.

Nevertheless the above-mentioned extensions of DFA show the need for a fluctuation analysis that can also handle oscillatory data automatically. The detrending procedure in DFA (Eq. (5)) can be regarded as a scale-dependent high-pass filter since (low-frequency) fluctuations exceeding a specific scale  $s$  are eliminated. Therefore, it has been suggested to obtain the detrended profile  $\tilde{X}_s(i)$  for each scale  $s$  directly by applying digital high-pass filters [45]. In particular, Butterworth, Chebyshev-I, Chebyshev-II, and an elliptical filter were suggested. While the elliptical filter showed the best performance in detecting long-range correlations in artificial data, the Chebyshev-II filter was found to be problematic. Additionally, in order to avoid a time shift between filtered and original profile, the average of the directly filtered signal and the time reversed filtered signal is considered. The effects of these complicated filters on the scaling behaviour are, however, not fully understood.

Finally, a continuous DFA method has been suggested in the context of studying heartbeat data during sleep [39,40]. The method compares unnormalized fluctuation functions  $F(s)$  for increasing length of the data. I.e., one starts with a very short recording and subsequently adds more points of data. The method is particularly suitable for the detection of change points in the data, e.g., physiological transitions between different activity or sleep stages. Since the main objective of the method is not the study of scaling behaviour, we do not discuss it in detail in this comparison.

### 3 Results

#### 3.1 Estimating the scaling behaviour in long and short data sets

In the first part of our comparison between DFA, CMA and MDFA, we calculate the scaling exponent  $\alpha$  for long-range correlated normally distributed data sets of length  $N = 50000$ . The data sets are generated using the modified Fourier filtering method, see, e. g., [49]. As one can see in Fig. 1(a), all three methods give sufficiently good results for different values of  $\alpha$ . However, on closer examination, i. e., looking at the successive slopes (logarithmic point to point derivatives) of  $F(s)$  (Figs. 1(b)-(d)), it can be seen that DFA1 and MDFA1 systematically overestimate the scaling exponent for small scales  $s$ . This effect has already been discussed for DFA and a modification was suggested for removing this artifact [8,50]. In addition, the significant fluctuations of the successive slopes of DFA1 (and MDFA1) on large scales  $s$ , led to the

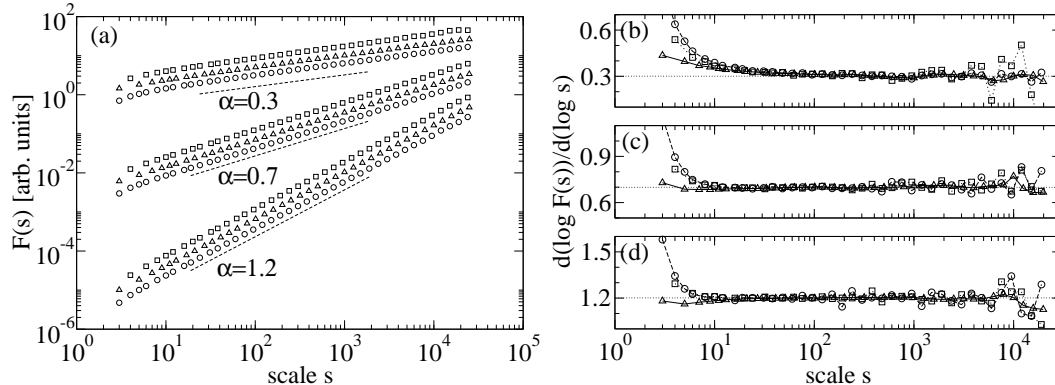


Fig. 1. (a) Fluctuation functions  $F(s)$  versus scale  $s$  of long-range correlated data with different scaling exponents  $\alpha = 0.3, 0.7, 1.2$ , by means of DFA1 (circles), CMA (triangles) and MDFA1 (squares). The results have been obtained by averaging  $F^2(s)$  over 100 artificial series of length  $N = 50000$  for each method and scaling exponent. The DFA1 curve is shifted downwards for clarity. (b)-(d) Point to point derivative of the average fluctuation functions shown in Fig. 1(a) for (b)  $\alpha = 0.3$ , (c)  $\alpha = 0.7$  and (d)  $\alpha = 1.2$ . Note the deviation from the scaling behaviour for small and large scales for DFA1 and MDFA1.

rule of determining  $\alpha$  only up to a scale of  $N/4$  [8]. Nevertheless, Figs. 1(b)-(d) show that the scaling behaviour of CMA is more stable than for DFA1 and MDFA1, suggesting that CMA could be used for reliable computation of  $\alpha$  even for scales  $s < 10$  and up to  $s_{\max} = N/2$ .

An important topic in fluctuation analysis is the influence of the signal length upon the reliability of the estimated scaling behaviour. For this purpose, we applied DFA1, CMA and MDFA1 on long-range correlated data and calculated the mean and standard deviation of the scaling exponents ( $\bar{\alpha}$ ,  $\sigma(\alpha)$ ) as function of the signal length  $N$  (Figs. 2 (a)-(c)). There are two ways in defining the scaling range for the fitting procedure of  $\alpha$ . Firstly one can fix the lower limit to  $s = 10$  (in order to reduce the influence of the small scales, where  $\alpha$  is overestimated by DFA1 and MDFA1, see Figs. 1(b)-(d)). The upper limit in this "fixed lower limit" range is set to  $N/2$  here. Figure 2 shows the result for this first definition. As can be clearly seen, the exponents become more accurate if a larger scaling range is used in the fitting procedure. While CMA and DFA1 show similar results and systematically underestimate the real scaling exponent for very short data ( $N < 100$ )<sup>2</sup>,  $\bar{\alpha}_{\text{MDFA}}$  is quite stable. However,

<sup>2</sup> This outcome is rather surprising, since from Fig. 1 one would expect that DFA1 and MDFA1 overestimate  $\alpha$  for short data (due to the deviations on small scales). However, it turns out that one has to take into account the different averaging procedures. In Fig. 2 we simply average over all calculated exponents for given data lengths, which have a large standard deviation for short series. On the other side, in Fig. 1, the fluctuation functions are averaged non-logarithmically. Configurations with large values thus affect the means much more than configurations with small values. This averaging procedure favours larger slopes, since the variations of  $F(s)$

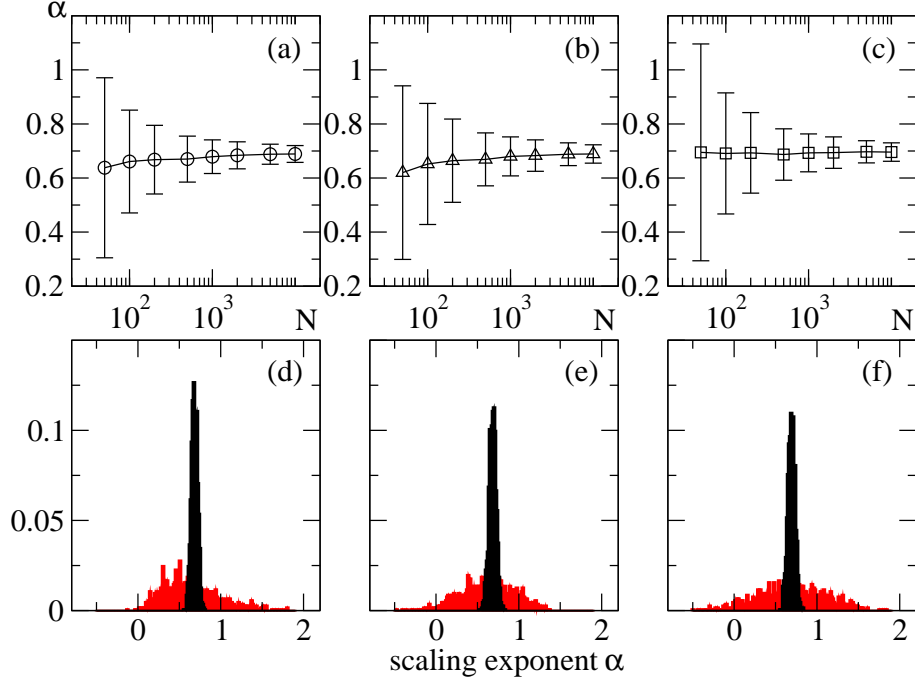


Fig. 2. (colour online) Mean and standard deviation of the calculated scaling exponents for different signal lengths  $N$  and histograms of scaling exponents. The fitting range was fixed at a lower limit namely  $s \in [10, N/2]$ . We applied (a) DFA1, (b) CMA and (c) MDFA1 to 1000 generated series with  $\alpha = 0.7$ . In (d)-(f), the corresponding normalized histograms of the scaling exponents are shown for  $N = 50$  (red colour) and  $N = 5000$  (black colour). Note that the distribution of  $\alpha_{\text{DFA}}$  is asymmetric for  $N = 50$ .

$\sigma(\alpha_{\text{MDFA}})$  is significantly increased for  $N < 100$  (see also Fig. 3).

An alternative definition of  $\alpha$  is based on a moving fitting regime with "fixed width", e.g., from  $N/20$  to  $N/2$ . In this case,  $\sigma(\alpha)$  is practically independent of  $N$  (not shown). Since both definitions are identical for  $N = 200$ , the results in Fig. 2 for  $N = 200$  are valid also for larger  $N$  in case of the fixed width definition. In the following, we will only refer to a fitting range with fixed lower limit.

An interesting question when studying the behaviour of  $\sigma(\alpha)$  versus  $N$  is whether the variations of  $\alpha$  are due to fluctuating properties of the data or due to the inaccuracy of the methods. It is hard to clarify this, since there is no way to identify or define a scaling exponent for any data without applying an analyzing method. Here we use DFA as such reference method. In the Fourier Filtering Method (see above) the data is generated by manipulating the slope in the power spectrum, i.e.  $\beta$ , which is directly related to the exponent  $\alpha$  (see Section 3.2 and [51]). Nevertheless, the shorter a time series, the less

---

are generally larger for larger  $s$ . Further on, the larger slopes occur for  $s < 10$  in Fig. 1(b), while the fitting range is set to  $10 \leq s \leq 25$  for the first point in Fig. 2(a).

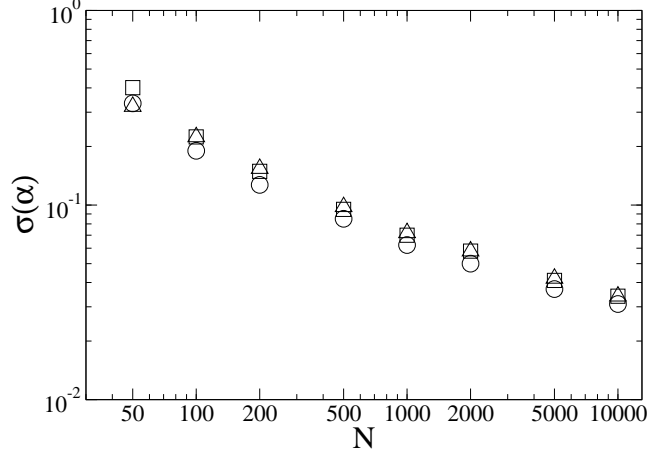


Fig. 3. Standard deviation of  $\alpha$  versus signal lengths  $N$  for DFA1 (circles), CMA (triangles) and MDFA1 (squares). This figure can be used as a calibration curve, i.e. to estimate the uncertainty,  $\sigma$ , of  $\alpha$  depending on the signal length  $N$ . For each method we averaged over 1000 series with  $\alpha = 0.7$ .

well-defined its intrinsic exponents  $\alpha$  and  $\beta$  become. The power spectrum and DFA fluctuation function become less smooth as a time series becomes shorter, increasing the error in calculating (and already defining) the exponents. The less smooth the curves are, the less accurate are the exponents defined and different methods will yield different results. This is essentially not an error in one or the other method.

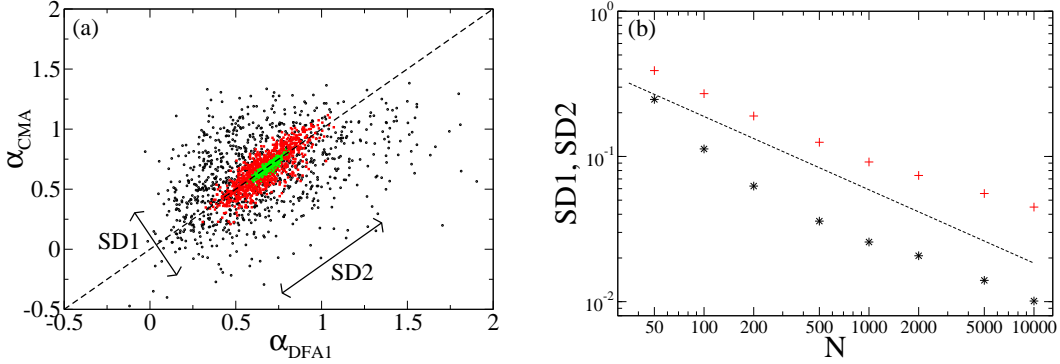


Fig. 4. (colour online) (a) Correlation scattering plots of the scaling exponents calculated with DFA1 and CMA for  $N = 50$  (black),  $N = 200$  (red) and  $N = 5000$  (green). (b) Corresponding standard deviations  $SD1$  (black stars) and  $SD2$  (red plus signs) as defined in Eqs. (10) versus  $N$ . Note that  $SD1$  decreases faster with  $N$  than  $SD2$ , suggesting that the uncertainty of CMA and DFA1 decreases faster with  $N$  than the indeterminacy of data generation; for comparison see the dotted line:  $SD \sim (\ln N)^{-1/2}$ . The results of 1000 series with an imposed value of  $\alpha = 0.7$  are shown.

In order to get an impression of the uncertainty of the methods and the error in generating data sets with a certain scaling exponent, one can study correlation scattering plots (Figs. 4 and 5). The standard deviations to characterize such

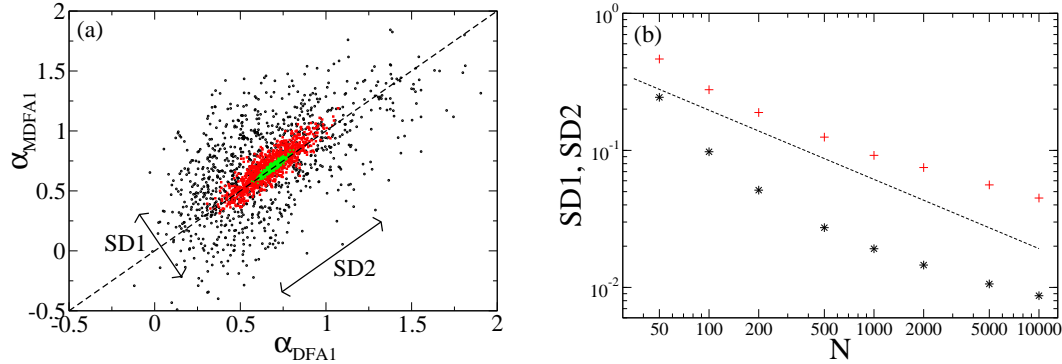


Fig. 5. (colour online) Same as Fig. 4 but for the scaling exponents calculated with DFA1 and MDFA1. Similar plots are obtained for CMA versus MDFA1 (not shown).

plots are defined by [52]

$$\begin{aligned}
 SD1 &= \sqrt{\frac{1}{N} \sum_{i=1}^N \frac{1}{2} [(\alpha_{\text{DFA}}^i - \alpha_y^i) - \langle \alpha_{\text{DFA}}^i - \alpha_y^i \rangle]^2}, \\
 SD2 &= \sqrt{\frac{1}{N} \sum_{i=1}^N \frac{1}{2} [(\alpha_{\text{DFA}}^i + \alpha_y^i) - \langle \alpha_{\text{DFA}}^i + \alpha_y^i \rangle]^2},
 \end{aligned} \tag{10}$$

so that  $SD1$  ( $SD2$ ) is the standard deviation perpendicular (parallel) to the line given by  $\alpha_{\text{DFA}} = \alpha_y$ , where  $\alpha_y$  is the scaling exponent calculated by method  $y$ . Assuming that  $\alpha_y$  is composed of the intrinsic scaling exponent  $\tilde{\alpha}_y$  of method  $y$  and an error  $\Delta\alpha$  because of data generation, it can be seen from Eq. (10) that  $SD1$  eliminates  $\Delta\alpha$  and thus may give a hint about the accuracy of method  $y$ .<sup>3</sup> If the considered method calculates exactly the same scaling exponent as DFA1,  $SD1$  would vanish. On the other hand, if method  $y$  deviates from DFA1,  $SD1$  will become large, i. e. comparable with  $SD2$ . Consequently, the indeterminacy of data generation can be assessed by the difference between  $SD2$  and  $SD1$ .

Figures 4 and 5 show that  $SD1$  is clearly smaller than  $SD2$  suggesting that the errors from data generation are larger than the deviations of both, CMA and MDFA1 results from DFA1 results. In addition the decay of  $SD1$  is faster than  $(\ln N)^{-1/2}$  while the decay of  $SD2$  is slower than this.

### 3.2 Determination of crossovers

An often observed phenomenon in real world data sets is the occurrence of crossovers, i.e., the correlations of the recorded data do not follow the same scaling law for all time scales  $s$ . Crossovers occur, for example, in the analysis

<sup>3</sup> Alternatively, if one does not compare method  $y$  to a reference method, such as DFA1 in this case, an additional error by estimating  $\alpha$  should be taken into account.

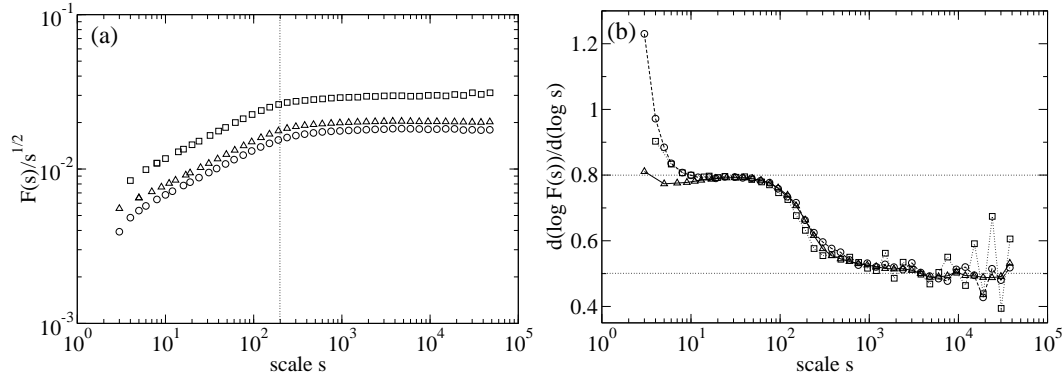


Fig. 6. (a) Fluctuation functions  $F(s)$  of DFA1 (circles), CMA (triangles) and MDFA1 (squares) versus time scales  $s$  for data with  $\alpha = 0.8$  for  $s < s_\times$  and  $\alpha = 0.5$  for  $s > s_\times$  (here  $s_\times = 200$ ). The results have been obtained by averaging 200 data series of length  $N = 100000$  for each method. Note that for the sake of clarity  $F(s)$  was divided by  $s^{1/2}$ . (b) Point to point derivative of  $F(s)$  shown in (a).

of short-term correlated data with finite decay time. Hence, an exact detection of crossovers is essential for finding characteristic time scales in complex systems. To compare the performance of DFA1, CMA, and MDFA1 regarding the detection of crossovers, we applied these methods to artificial time series with a well-defined crossover at scale  $s_\times$ . The results are shown in Fig. 6.

It is sufficient to study only one scenario of a crossover in artificial data since the systematic deviation of the observed crossover from the real crossover was found to be independent of the values of  $\alpha$  for DFA [8]. A convenient way to generate such time series is by using a modification of the Fourier filtering method. If we need a crossover at scale  $s_\times$  with scaling exponents  $\alpha_1$  for  $s < s_\times$  and  $\alpha_2$  for  $s > s_\times$ , the power spectrum of an uncorrelated random series is multiplied by  $(f/f_\times)^{-\beta_2}$  for low frequencies  $f < f_\times = 1/s_\times$  and with  $(f/f_\times)^{-\beta_1}$  for frequencies  $f > f_\times$ . The relation between  $\alpha$  and  $\beta$  is given by  $\beta = 2\alpha - 1$  [51]; the inverse Fourier transform of the manipulated power spectrum yields the desired data.

Figure 7 shows our results for generated data with systematically varied real crossover  $s_\times$ . While DFA1 and CMA slightly overestimate the position of the crossover ( $s'_\times > s_\times$ ) by the same degree, MDFA detects  $s_\times$  rather accurately. Clearly, a linear relationship between  $s_\times$  and  $s'_\times$  is observed. Hence, when observing a crossover at position  $s'_\times$  in DFA1, CMA, or MDFA1, the real crossover position  $s_\times$  can be estimated by the equations given in the caption of Fig. 7.

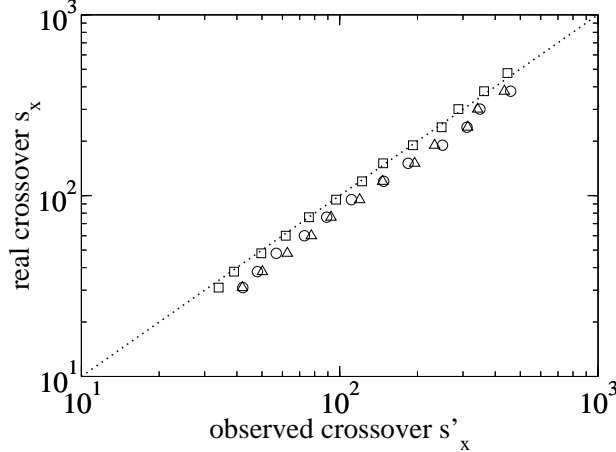


Fig. 7. Real crossovers  $s_x$  versus observed crossovers  $s'_x$  for DFA1 (circles), CMA (triangles) and MDFA1 (squares). The results have been obtained by averaging over the same number of configurations as in Fig. 6 for each  $s_x$ . The  $s_x$  values can be estimated from  $s'_x$  by  $\ln s_x \approx \ln s'_x - 0.25$  (DFA1),  $\ln s_x \approx 1.05 \ln s'_x - 0.47$  (CMA), and  $\ln s_x \approx 1.04 \ln s'_x - 0.19$  (MDFA1), respectively.

### 3.3 Data with monotonous trends

Trends are ubiquitous in many noisy signals obtained from real systems. As it was discussed above and shown in previous work, trends may mask the real correlation behaviour of the intrinsic fluctuations in the data. To study the effect of trends in DFA, CMA and MDFA, we have added a linear and a non-integer trend to the original record ( $x_i$ ) generated with the Fourier transform method. Other kinds of trends (polynomial, sinusoidal and irregularly oscillating) have been systematically studied elsewhere [8,9,42,43,44].

Figure 8 depicts our results after adding a linear trend to long-range correlated data (with  $\langle x \rangle = 0$  and  $\sigma(x) = 1$  before adding the trend). Since DFA1, CMA and MDFA1 are, by definition, not able to remove linear trends in the original data, all  $F(s)$  curves show trend induced crossovers at  $s'_x$ , which occur slightly earlier for MDFA1. Above the crossover, an artificial scaling exponent  $\alpha_{\text{trend}} = 2$  is observed in agreement with [8]. A systematic variation of the strength of the trend  $A$  shows that the crossover position  $s'_x$  increases with  $A$  as  $s'_x \sim A^{-\delta}$  with an exponent  $\delta \approx 0.71$ , independent of the technique (see inset of Fig. 8(a)) and also independent of the fluctuation exponent  $\alpha$  (not shown). This scaling relation allows to extrapolate for smaller values of  $A$ . For comparison, the fluctuation function  $F(s)$  is also shown for DFA2. In this case, we clearly observe the expected scaling behaviour without any crossover.

The application of a non-integer trend, e. g.  $x'_i = x_i + A(i/N)^{1.2}$  leads to similar results as shown in Fig. 8 (not shown, see also [8] for DFA). However, here we also observe a trend related crossover for DFA2.



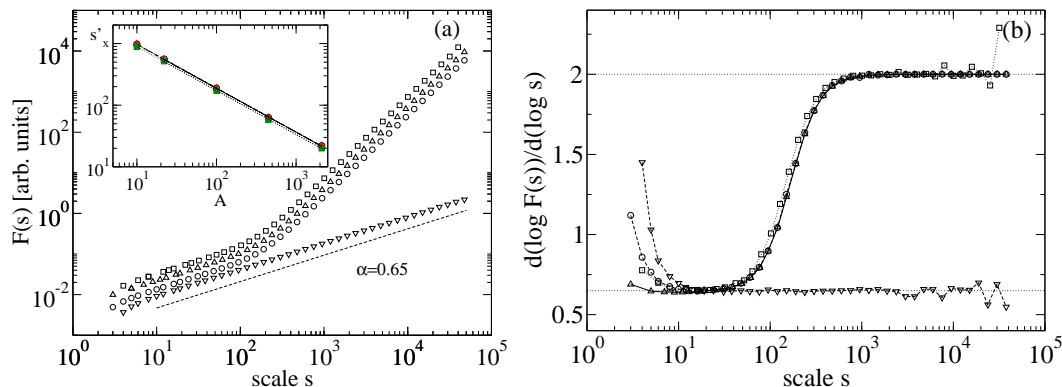


Fig. 8. Fluctuation functions and point to point derivative of long-range correlated data sets with a linear trend:  $x'_i = x_i + Ax$  with  $x = i/N$  ( $\alpha = 0.65$ ,  $A = 10$ ). (a) Trend-related crossover after analysis by means of DFA1 (circles,  $s'_x \approx 187$ ), CMA (triangles up,  $s'_x \approx 186$ ) and MDFA1 (squares,  $s'_x \approx 170$ ). For comparison,  $F(s)$  versus  $s$  is shown also for DFA2 (triangles down). Since DFA2 eliminates the linear trend in  $x'_i$  we find the expected scaling behaviour  $F(s) \sim s^{0.65}$  without crossover (the DFA curves were shifted downwards for better visibility). In the inset the position of the crossover is shown for different strengths  $A$  of the trend for all three methods; the data can be fitted by  $s'_x \propto A^{-\delta}$  with an exponent  $\delta \approx 0.71$ , independent of the technique. (b) Point to point derivative of the  $F(s)$  functions shown in (a). The results were obtained by averaging 100 data series of length  $N = 100000$ .

## 4 Conclusion

In summary, we have compared several recently suggested detrending methods based on random walk theory which were developed to detect long-range correlations in data affected by trends. In particular, we investigated the performance of the Centered Moving Average (CMA) method and the Modified Detrended Fluctuation Analysis (MDFA) regarding their behaviour on small and large scales, and the determination of crossovers in monofractal data sets with different lengths and monotonous trends. A systematic comparison of CMA and MDFA with standard DFA showed a small advantage of CMA in the computation of the scaling behaviour on small ( $s < 10$ ) and large ( $s > N/4$ ) scales. The detection of crossovers in the data was somewhat more exact with MDFA. Ultimately, we think that CMA is a good alternative to DFA1 when analyzing the scaling properties in short data sets without trends. Nevertheless for data with possible unknown trends we recommend the application of standard DFA with several different detrending polynomial orders to distinguish real crossovers from artificial crossovers due to trends. In addition, an independent approach (e.g., wavelet analysis) should be used to confirm findings of long-range correlations.

*Acknowledgement:* We thank Diego Rybski for very helpful discussions. This work has been supported by the Deutsche Forschungsgemeinschaft (grant KA 1676/3) and the European Union (STREP project DAPHNet, grant 018474-2). RB acknowledges financial support from the President scholarship of Bar-Ilan University.

## References

- [1] C.-K. Peng, S.V. Buldyrev, S. Havlin, M. Simons, H.E. Stanley, and A.L. Goldberger, *Phys. Rev. E* **49**, 1685 (1994).
- [2] H.E. Hurst, *Transactions of the American Society of Civil Engineering* **116**, 770 (1951).
- [3] C.-K. Peng, S.V. Buldyrev, A.L. Goldberger, S. Havlin, F. Sciortino, M. Simons, and H.E. Stanley, *Nature* **356**, 168 (1992).
- [4] A. Bunde, S. Havlin, J.W. Kantelhardt, T. Penzel, J.-H. Peter, and K. Voigt, *Phys. Rev. Lett.* **85**, 3736 (2000).
- [5] J.W. Kantelhardt, S.A. Zschiegner, A. Bunde, S. Havlin, E. Koscielny-Bunde, and H.E. Stanley, *Physica A* **316**, 87 (2002).
- [6] Y. Ashkenazy, P.Ch. Ivanov, S. Havlin, C.-K. Peng, A.L. Goldberger, and H.E. Stanley, *Phys. Rev. Lett.* **86**, 1900 (2001).
- [7] G.-F. Gu and W.-X. Zhou, *Phys. Rev. E* **74**, 061104 (2006)
- [8] J.W. Kantelhardt, E. Koscielny-Bunde, H.H.A. Rego, S. Havlin, and A. Bunde, *Physica A* **295**, 441 (2001).
- [9] K. Hu, P.Ch. Ivanov, Z. Chen, P. Carpena, and H.E. Stanley, *Phys. Rev. E* **64**, 011114 (2001).
- [10] Z. Chen, P.Ch. Ivanov, K. Hu, and H.E. Stanley, *Phys. Rev. E* **65**, 041107 (2002).
- [11] Z. Chen, K. Hu, P. Carpena, P. Bernaola-Galvan, H.E. Stanley, and P.Ch. Ivanov, *Phys. Rev. E* **71**, 011104 (2005).
- [12] P. Grau-Carles, *Physics A* **360**, 89 (2006).
- [13] R. Nagarajan, *Physica A* **363**, 226 (2006).
- [14] M.S. Taqqu, V. Teverovsky, and W. Willinger, *Fractals* **3**, 785 (1995).
- [15] C. Heneghan and G. McDarby, *Phys. Rev. E* **62**, 6103 (2000).
- [16] R. Weron, *Physica A* **312**, 285 (2002).
- [17] J. Mielniczuk and P. Wojdylo, *Comp. Stat. Data. Anal.* **51**, 4510 (2007).

- [18] D. Delignieres, S. Ramdani, L. Lemoine, K. Torre, M. Fortes, and G. Ninot, *J. Math. Psychol.* **50**, 525 (2006).
- [19] S. Bahar, J.W. Kantelhardt, A. Neiman, H.H.A. Rego, D.F. Russell, L. Wilkens, A. Bunde, and F. Moss, *Europhys. Lett.* **56**, 454 (2001).
- [20] R. Bartsch, T. Henning, A. Heinen, S. Heinrichs, and P. Maass, *Physica A* **354**, 415 (2005).
- [21] M.S. Santhanam, J.N. Bandyopadhyay, and D. Angom, *Phys. Rev. E* **73**, 015201 (2006).
- [22] T. Barnett, F. Zwiers, G. Hegerl, M. Allen, T. Crowley, N. Gillett, K. Hasselmann, P. Jones, B. Santer, R. Schnur, P. Scott, K. Taylor, and S. Tett, *J. of Climate* **18**, 1291 (2005).
- [23] E. Koscielny-Bunde, A. Bunde, S. Havlin, H.E. Roman, Y. Goldreich, and H.J. Schellnhuber, *Phys. Rev. Lett.* **81**, 729 (1998).
- [24] J.W. Kantelhardt, D. Rybski, S.A. Zschiegner, P. Braun, E. Koscielny-Bunde, V. Livina, S. Havlin, and A. Bunde, *Physica A* **330**, 240 (2003).
- [25] E. Koscielny-Bunde, J.W. Kantelhardt, P. Braun, A. Bunde, and S. Havlin, *J. Hydrol.* **322**, 120 (2006).
- [26] J.W. Kantelhardt, E. Koscielny-Bunde, D. Rybski, P. Braun, A. Bunde, and S. Havlin, *J. Geophys. Res. (Atmosph.)* **111**, D01106 (2006).
- [27] R. Karasik, N. Sapir, Y. Ashkenazy, P.Ch. Ivanov, I. Dvir, P. Lavie, and S. Havlin, *Phys. Rev. E* **66**, 062902 (2002).
- [28] L.-M. Stadler, B. Sepiol, J.W. Kantelhardt, I. Zizak, G. Grübel, and G. Vogl, *Phys. Rev. B* **69**, 224301 (2004).
- [29] D.T. Schmitt and M. Schulz, *Phys. Rev. E* **73**, 056204 (2006).
- [30] E. Giese, I. Mossig, D. Rybski, and A. Bunde, *Erdkunde* **61**, 186 (2007).
- [31] B. Audit, E. Bacry, J.F. Muzy, and A. Arneodo, *IEEE Transact. Inform. Th.* **48**, 2938 (2002).
- [32] M. Ignaccolo, P. Allegrini, P. Grigolini, P. Hamilton, and B.J. West, *Physica A* **336**, 595 (2004).
- [33] F. Principato and G. Ferrante, *Physica A* **380**, 75 (2007).
- [34] E. Alessio, A. Carbone, G. Castelli, and V. Frappietro, *Europ. Phys. J. B* **27**, 197 (2002).
- [35] A. Carbone, G. Castelli, and H.E. Stanley, *Phys. Rev. E* **69**, 026105 (2004).
- [36] A. Carbone, G. Castelli, and H.E. Stanley, *Physica A* **344**, 267 (2004).
- [37] J. Alvarez-Ramirez, E. Rodriguez, and J.C. Echeverría, *Physica A* **354**, 199 (2005).

- [38] K. Kiyono, Z.R. Struzik, N. Aoyagi, F. Togo, and Y. Yamamoto, *Phys. Rev. Lett.* **95**, 058101 (2005).
- [39] M. Staudacher, S. Telser, A. Amann, H. Hinterhuber, and M. Ritsch-Marte, *Physica A* **349**, 582 (2005).
- [40] S. Telser, M. Staudacher, B. Hennig, Y. Ploner, A. Amann, H. Hinterhuber, and M. Ritsch-Marte, *J. Biol. Phys.* **33**, 19 (2007).
- [41] C.V. Chianca, A. Ticona, and T.J.P. Penna, *Physica A* **357**, 447 (2005).
- [42] I.M. Jánosi and R. Müller, *Phys. Rev. E* **71**, 056126 (2005).
- [43] R. Nagarajan and R.G. Kavasseri, *Physica A* **354**, 182 (2005).
- [44] R. Nagarajan, *Physica A* **366**, 1 (2006).
- [45] E. Rodriguez, J.C. Echeverria, and J. Alvarez-Ramirez, *Physica A* **375**, 699 (2007).
- [46] D. Grech and Z. Mazur, *Acta Phys. Pol. B* **36**, 2403 (2005).
- [47] L. Xu, P.Ch. Ivanov, K.Hu, Z. Chen, A. Carbone, and H.E. Stanley, *Phys. Rev. E* **71**, 051101 (2005).
- [48] P. Oswiecimka, J. Kwapien, and S. Drozd, *Phys. Rev. E* **74**, 016103 (2006).
- [49] H.A. Makse, S. Havlin, M. Schwartz, and H. E. Stanley, *Phys. Rev. E* **53**, 5445 (1996).
- [50] R. Bartsch, M. Plotnik, J.W. Kantelhardt, S. Havlin, N. Giladi, and J.M. Hausdorff, *Physica A* **383**, 455 (2007).
- [51] S. Havlin, R.B. Selinger, M. Schwartz, H.E. Stanley, and A. Bunde, *Phys. Rev. Lett.* **61**, 1438 (1988).
- [52] J. Piskorski and P. Guzik, *Physiol. Meas.* **28**, 287 (2007).